

Modeling of Industrial Accidents with Liquefied Toxic and Flammable Gases

A. A. Kuleshov^a, N. M. Hidalgo Dias^a, G. M. Makhviladze^b, and S. E. Yakush^c

^a *Institute for Mathematical Modeling, Russian Academy of Sciences, Moscow, 125047 Russia*
e-mail: andrew_kuleshov@mail.ru

^b *University of Central Lancashire, Preston, United Kingdom*

^c *Ishlinskii Institute for Problems in Mechanics, Russian Academy of Sciences, Moscow, Russia*

Received October 26, 2009

Abstract—Modeling of industrial accidents with liquefied toxic and flammable gases is considered. Propagation of nonreacting heavy gas clouds over complex terrains is described by a two-dimensional model with averaging over the cloud height. A numerical simulation of a toxic accident initiated by the release of chlorine in the urban environment has been performed and the number of injured people has been computed. A two-dimensional axisymmetric model based on the Favre-averaged Navier–Stokes equations is used to model the fireballs occurring upon combustion of hydrocarbon fuel-air clouds. Zones of various thermal hazards for people have been obtained.

Keywords: industrial accidents, toxic and flammable gases, heavy gas clouds propagation, fireball, consequence analysis, numerical simulation.

DOI: 10.1134/S2070048210060049

INTRODUCTION

Accidents at objects of transportation and storage of liquefied toxic and flammable gases cause a great danger both for the personnel of these objects and for the population of adjacent regions, as well as a great deal of economic damage [1]. Therefore, research on such accidents is very urgent. As long as full-scale natural experiments remain difficult to implement, the method of mathematical modeling, which can predict the dynamics of probable accidents and estimate their possible consequences, remains the basic research tool that can be used. Also mathematical modeling allows one to reconstruct events and analyze accidents that have already occurred.

Two types of technogenic accidents with liquefied gases will be considered below: accidents with toxic heavy gases for which the modeling is carried out of the distribution of the formed air-gas cloud under the influence of gravity and wind in urban environment with detection of the toxic damage to people, and accidents with the combustion of fuel-air clouds in a fireball mode with calculation of thermal damage zones.

The flammable and toxic gases stored in a liquefied state at increased pressure and ambient temperature are considered in the work as dangerous substances. Upon depressurization of a tank or pipeline, the liquefied gas almost instantly evaporates from the overflow and forms a cloud of an air-gas mixture. The so-called heavy gases of which the true density at atmospheric pressure is over air density are considered in the work. This is a wide enough class of dangerous gases to which all combustible oil gases belong, such as propane, butane and their mixtures, and the most widely used toxic gas in industrial production, chlorine. In modeling fireballs, butane is considered as a fuel in the present work.

Turbulent flows arising during real emergency emissions have a complex three-dimensional character that essentially complicates their numerical modeling. However, for an operative estimation of the development of emergencies, specific models are needed. Using these models, fast calculations of the dynamics of technogenic accidents can be conducted on personal computers and their consequences can be estimated. In the development of such models, it is expedient to use simplified two-dimensional problem statements taking into account the features appropriate to flows of various types. For the reduction of the spatial problem to a two-dimensional one, in the models of the distribution of heavy nonreacting gas clouds, an averaging on the applicate has been carried out, while for the burning of clouds, the influence of wind is neglected and an assumption on the flow's symmetry about the vertical axis is introduced.

1. MODELING OF TOXIC ACCIDENTS WITH LIQUEFIED GASES

Mathematical model. For the description of the propagation of heavy gas clouds over a complex underlying surface the two-dimensional model [2, 3] constructed by the averaging method on the height of the flow of the initial three-dimensional hydrodynamics equations in Euler variables, which was developed earlier, has been used. This model is a generalization of the well-known flow model of an incompressible liquid of a free surface—the model of shallow water [4] in the case of hydrodynamic flows with variable density and variable mass concentration of components of a gaseous medium. These parameters allow one to judge whether the maximum permissible concentrations (MPCs) in a cloud have been attained, and to estimate the probability of toxic damage to personnel on industrial objects and the population in adjacent housing areas.

The system of equations of the two-dimensional model [2, 3] is considered in Cartesian coordinates in a rectangular area $\Omega = \{0 \leq x \leq l_1, 0 \leq y \leq l_2\}$ on a horizontal plane XY :

$$\frac{\partial \bar{\rho} \delta}{\partial t} + \frac{\partial \bar{\rho} \bar{u} \delta}{\partial x} + \frac{\partial \bar{\rho} \bar{v} \delta}{\partial y} = Q, \quad (1.1)$$

$$\frac{\partial \bar{\rho} \bar{u} \delta}{\partial t} + \frac{\partial \bar{\rho} \bar{u}^2 \delta}{\partial x} + \frac{\partial \bar{\rho} \bar{u} \bar{v} \delta}{\partial y} = -\frac{g \delta^2}{2} \frac{\partial \bar{\rho}}{\partial x} - g(\bar{\rho} - \rho_0) \delta \frac{\partial(z_0 + \delta)}{\partial x} + \frac{\partial \bar{\tau}_{xx}}{\partial x} + \frac{\partial \bar{\tau}_{yx}}{\partial y} + \bar{F}_1 + F_{1H} + F_{1z_0}, \quad (1.2)$$

$$\frac{\partial \bar{\rho} \bar{v} \delta}{\partial t} + \frac{\partial \bar{\rho} \bar{u} \bar{v} \delta}{\partial x} + \frac{\partial \bar{\rho} \bar{v}^2 \delta}{\partial y} = -\frac{g \delta^2}{2} \frac{\partial \bar{\rho}}{\partial y} - g(\bar{\rho} - \rho_0) \delta \frac{\partial(z_0 + \delta)}{\partial y} + \frac{\partial \bar{\tau}_{xy}}{\partial x} + \frac{\partial \bar{\tau}_{yy}}{\partial y} + \bar{F}_2 + F_{2H} + F_{2z_0}, \quad (1.3)$$

$$\frac{\partial \bar{\rho} \bar{C} \delta}{\partial t} + \frac{\partial \bar{\rho} \bar{u} \bar{C} \delta}{\partial x} + \frac{\partial \bar{\rho} \bar{v} \bar{C} \delta}{\partial y} = \frac{\partial}{\partial x} \left(D_t \frac{\partial \bar{C} \delta}{\partial x} \right) + \frac{\partial}{\partial y} \left(D_t \frac{\partial \bar{C} \delta}{\partial y} \right) + J_C + Q_C, \quad (1.4)$$

$$\bar{\rho} = \frac{\rho_0}{1 + (M_0/M - 1) \bar{C}}, \quad (1.5)$$

where $\bar{\rho}$, \bar{u} , \bar{v} , and \bar{C} are the density, components of velocity $\bar{\mathbf{V}} = (\bar{u}, \bar{v})^T$, and relative mass concentration of gas that are averaged over cloud thickness δ , which is also defined in the system's solution (1.1)–(1.5). The pressure gradient in Eqs. (1.2) and (1.3) is expressed through the terms with gradients of density, cloud thickness and the function $z_0(x, y)$, specifying the relief of the underlying surface, g is the acceleration of gravity, M is the molecular weight of the gas, and ρ_0 and M_0 are, respectively, the density and molecular weight of the surrounding atmospheric air. The entry of gas from surface sources in (1.1) and (1.4) is specified by the source terms Q and $Q_C = C_0 Q$, where C_0 is the relative mass concentration of gas on a surface source. The tensor components of viscous pressures averaged by cloud thickness are

$$\bar{\tau}_{ik} = \mu_t \left(\frac{\partial \bar{V}_i \delta}{\partial x_k} + \frac{\partial \bar{V}_k \delta}{\partial x_i} \right), \quad i, k = 1, 2, \quad x_1 = x, \quad x_2 = y, \quad \bar{V}_1 = \bar{u}, \quad \bar{V}_2 = \bar{v}; \quad (1.6)$$

for the coefficient of turbulent viscosity, the two-dimensional analogue of the model [5] has been used

$$\mu_t = \frac{\bar{\rho} l^2}{2} \left\{ \left(\frac{\partial \bar{u}}{\partial y} + \frac{\partial \bar{v}}{\partial x} \right)^2 + 2 \left[\left(\frac{\partial \bar{u}}{\partial x} \right)^2 + \left(\frac{\partial \bar{v}}{\partial y} \right)^2 \right] \right\}^{1/2}, \quad (1.7)$$

where the mixing length l is assumed to be equal to the cloud's thickness $l = \delta(x, y, t)$. The coefficient of turbulent diffusion is defined by the formula $D_t = \mu_t / Sc_t$, where $Sc_t = 0.7$ is the turbulent Schmidt number. The cloud's interaction with the environment is described by the source terms in Eqs. (1.2)–(1.4), where $\bar{\mathbf{F}} = -\xi \delta \bar{\rho} \bar{\mathbf{V}} |\bar{\mathbf{V}}|$ and $\bar{\mathbf{F}} = (\bar{F}_1, \bar{F}_2)^T$ are the volume of the frictional force of the cloud's substance on a surface of obstacles; $\xi = c_d s$ [m^{-1}] is the friction coefficient, including the constant of aerodynamic resistance c_d (taking into consideration the roughness of the surface of obstacles) and the specific surface of obstacles s [m^{-1}] in the considered volume of the environment; \mathbf{F}_H is the force of friction of the cloud's substance and atmospheric air on the upper boundary of the cloud in the presence of wind, which has a velocity of $\mathbf{V}_0 = (u_0, v_0)$; $\mathbf{F}_H = -\xi_0 \rho_0 (\bar{\mathbf{V}} - \mathbf{V}_0) |\bar{\mathbf{V}} - \mathbf{V}_0|$; $\mathbf{F}_H = (F_{1H}, F_{2H})^T$; ξ_0 is the dimensionless empirical friction of cloud substance and atmospheric air on the upper boundary of the cloud; \mathbf{F}_{z_0} is the force of friction of the

Table

T	0.05	0.1	0.2	0.3	0.4	0.5	0.6	0.7	0.8	0.9
P	0.001	0.003	0.01	0.02	0.035	0.06	0.10	0.20	0.30	0.40
T	1	1.5	2	2.5	3	3.5	4	4.5	5	>5
P	0.50	0.67	0.79	0.87	0.92	0.95	0.97	0.98	0.99	1.0

cloud’s substance on the underlying surface $\mathbf{F}_{z_0} = -\xi_1 \bar{\rho} \bar{\mathbf{V}} |\bar{\mathbf{V}}|$; $\mathbf{F}_{z_0} = (F_{1z_0}, F_{2z_0})^T$; and ξ_1 is the dimensionless friction coefficient, which takes into consideration the roughness of the underlying surface. The source member J_C describes the dilution of gas in a cloud by the surrounding air due to turbulent diffusion on the upper boundary of cloud $J_C = -\xi_0 \rho_0 |\bar{\mathbf{V}} - \mathbf{V}_0| \bar{C}$.

Boundary and Initial Conditions

For the system of equations averaged by the height, the boundary conditions are specified on the open lateral boundary only: $\frac{\partial \Phi}{\partial n} \Big|_{\Gamma} = 0$, $\Phi = (\bar{\rho}, \bar{u}, \bar{v}, \bar{C})$, n is a normal to the Γ boundary of area Ω .

The initial values of parameters outside the initial cloud are parameters of the environment; and in the initial cloud, the relative mass concentration of gas \bar{C}^0 is set at the initial time, and the value of the gas density $\bar{\rho}^0$ is found from state Eq. (1.5); the initial velocity in the cloud is assumed to be zero $\bar{\mathbf{V}}^0 = 0$.

Thus, model (1.1)–(1.7) considers all the basic physical phenomena occurring in the considered process: gravitational spreading, turbulence, friction against the underlying surface and obstacles, cloud dilution by the air on the upper boundary, and the presence of wind.

Assessment technique of toxic damage at chemical accidents. In the estimation of toxic damage, technique [6] has been applied. Due to numerical modeling by the two-dimensional model of the propagation of heavy gas clouds (1.1)–(1.7), the fields of average values of the height of concentration $\bar{C}(x, y, t)$ and gas density $\bar{\rho}(x, y, t)$ in a cloud, as well as the cloud height $\delta(x, y, t)$, are determined. The relative mass concentration of gas, averaged by height, in a cloud of an air-gas mixture is $\bar{C} = \bar{\rho}_G / \bar{\rho}$, where $\bar{\rho}_G$ [g/m³] is the averaged partial gas density (gas weight in volume units). Then, knowing \bar{C} and $\bar{\rho}$, we find $\bar{\rho}_G = \bar{\rho} \bar{C}$. Knowing $\bar{\rho}_G(x, y, t)$, we can calculate the distribution field of toxic doses $D(x, y, t)$ [g s/m³] in time t by the formula $D(x, y, t) = \int_0^t \bar{\rho}_G(x, y, \tau) d\tau$; moreover, in the integral calculation, these time intervals are considered only when the cloud thickness is sufficient to reach human respiratory organs: $\delta(x, y, t) \geq H_D$.

The distribution field of toxic effects is calculated on the basis of the distribution field of toxic doses. $\mathbf{T} = (T_0, T_1, T_2, T_3, T_4)$ is a dimensionless five-component vector according to the degree of damage to a person: 0 corresponds to a deadly degree; 1, to a heavy degree; 2, to an average degree; 3, to a light degree; and 4, to a threshold degree, the components of which are determined by the formula $T_k(x, y, t) = D(x, y, t) / D_k^{50}$, $k = \overline{0, 4}$, where $\mathbf{D}^{50} = (D_0^{50}, D_1^{50}, D_2^{50}, D_3^{50}, D_4^{50})$ is a vector of average toxic doses causing the corresponding degree of damage on a person. For example, for chlorine, the vector of average doses is equal to $\mathbf{D}_{Cl_2}^{50} = (1726, 1086, 734, 382, 126)$ [g s/m³].

Then, the field of the probability of damage is determined according to the values of the field of toxic effects; $\mathbf{P}(x, y, t)$, $\mathbf{P} = (P_0, \dots, P_4)$ is also a five-component vector field according to the degrees of damage to a person $P_k(x, y, t) = F[T_k(x, y, t)]$, where the function F is given in the table.

The distribution of the probability of damage to people on the damage area (the coordinate law of damage) characterizes damage scales at a chemical accident.

On the basis of the coordinate law of damage, the reduced damage zone $S^P(t)$ is determined as an integral from the field of the damage probability on the damage area $S(t)$:

$$S^P(t) = \int_{S(t)} P(x, y, t) dx dy, \quad S^P(t) = (S_0^P, \dots, S_4^P).$$

The reduced damage zone is a basic characteristic of the hazardous effect of toxic substances at chemical accidents. The values of medical-sanitary consequences are defined by using values of the reduced damage zone calculated for different levels of damage to people: the values of irretrievable losses (lethal damages) and sanitary losses (damages of different levels: heavy, average, light, and threshold damages).

Let $n(t)$ be the number of people at time t located in the damage area $S(t)$, then $N(t) = n(t)/S(t)$ is the density of people in the damage zone. The number of people injured according to the degrees of damage is determined as a product of the density of the people in the reduced damage zone for the corresponding damage degree

$$N^P(t) = N(t)S^P(t), \quad N^P = (N_0^P, \dots, N_4^P).$$

On the basis of the algorithm of the numerical solution of problem (1.1)–(1.7), which was developed earlier, based on the split method according to the physical processes with the solution of the subsystem of equations arising by the difference method on rectangular grids (see [2, 3]), a new version of the program complex in the C++ language was created. A module for the calculation of toxic damage at chemical accidents by the technique stated above was included in the program complex.

Results of the numerical modeling of an accident with chlorine distribution. The modeling of the distribution of a chlorine cloud in a city building complex was carried out in the absence of wind. The model covers a square area of $500 \times 500 \text{ m}^2$ representing a fragment of the city building complex; the height of buildings varies between 20 and 30 m. The source, in the shape of a cylinder with a height of 15 m and a diameter of 50 m, is located in the center of the region. The relative mass concentration of chlorine in the source at the initial time moment is 10%, and there is no wind. The density of people on the terrain is equal to 1 person/50 m^2 , and there are 5000 persons in total.

The shape of the cloud at the initial time is shown in Fig. 1a and the results of the calculations are shown in Figs. 1b, 1c, and 1d: the cloud boundary (an external contour) and probability distribution of a deadly damage to people [P0] (internal contours) at time moments of 10, 35, and 50 s. The current velocity field is shown by vectors. The toxic damage to people is calculated when the cloud thickness exceeds $H_D = 1 \text{ m}$.

The dependence of the number of injured people with different injury levels on time is presented in Fig. 2. It is clear that at the given initial chlorine concentration (10%), the death-toll considerably exceeds the number of people with other damage degrees.

2. MODELING OF BURNING OF FUEL-AIR CLOUDS

Let us consider the processes occurring at the combustion of fuel-air clouds formed as a result of the destruction of a tank with hydrocarbon fuel under a high pressure.

The destruction of the cover of a tank with liquefied gas leads to a release of the energy of the boiling liquid and the formation of a two-phase steam-drop cloud accompanied by strong stream turbulization. As the experiments show, at the explosive boiling of liquefied oil gases, drops of 10–100 μm in diameter are formed; the evaporation of fuel drops in a saturated cloud is controlled by the processes of turbulent mixing with air and occurs for a much shorter time than the burning of the cloud [8, 9] (for typical accidents, the burning of fuel in the shape of a fireball varies from several seconds to 10 to 20 seconds, whereas the complete evaporation time period of small drops of liquefied propane is shorter by an order of magnitude). Therefore, a single-phase model of the process, which significantly simplifies numerical calculations, is considered in the work [10, 11].

Mathematical model. The burning of the cloud of a fuel-air mixture formed at the instant destruction of a high pressure tank is modeled by solving two-dimensional axisymmetric Navier–Stokes equations averaged according to Favre, and which are closed through the use of the standard $k - \varepsilon$ turbulence model (see [8–11]). The system of the determined equations has the following form:

$$\frac{\partial \rho}{\partial t} + \nabla(\rho \mathbf{U}) = 0, \quad (2.1)$$

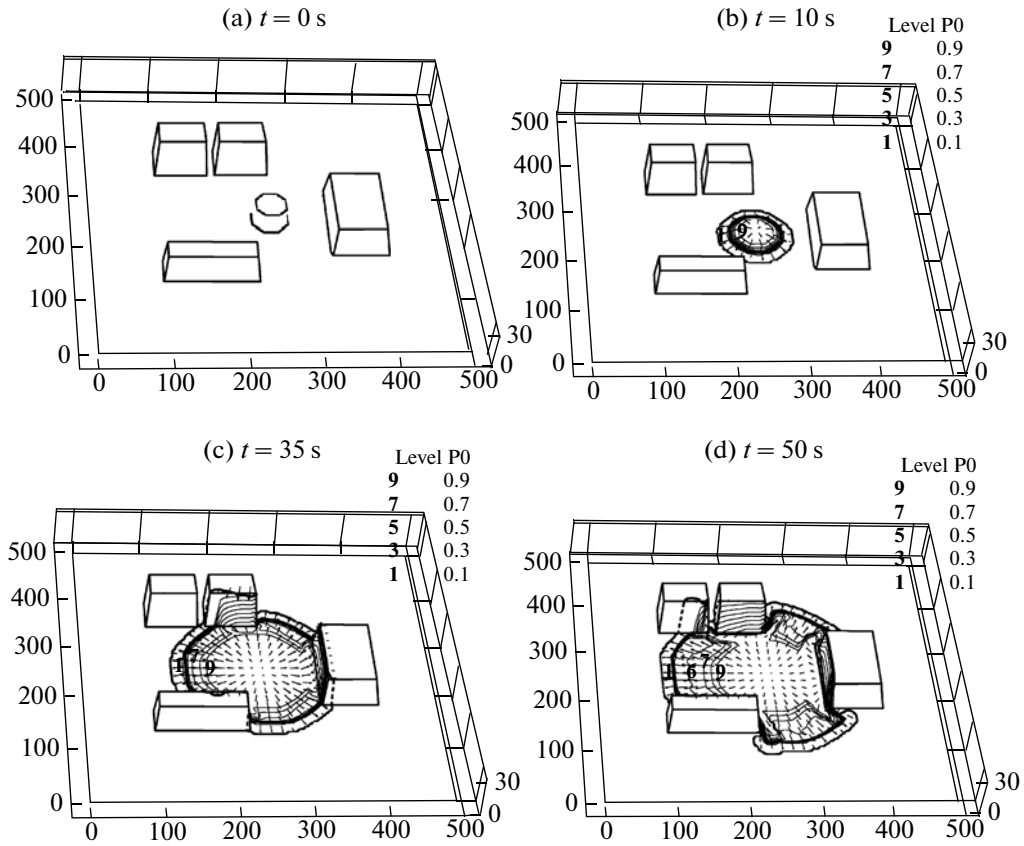


Fig. 1. The boundary of a cloud of a gas-air mixture (external contour) and the probability of a deadly damage to people P0 at times $t = 0, 10, 35,$ and 50 s.

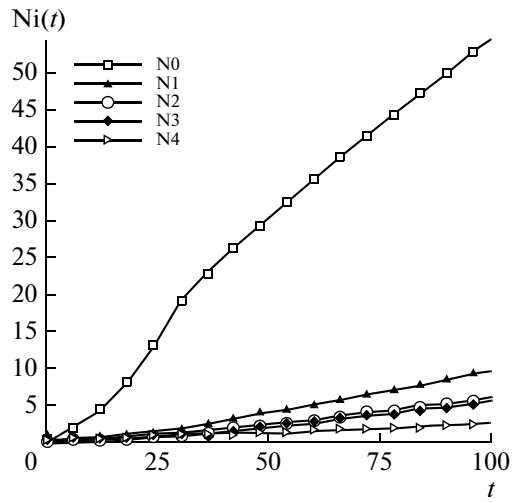


Fig. 2. Number of people with toxic damages of different degrees.

$$\frac{\partial \rho \mathbf{U}}{\partial t} + \nabla \cdot (\rho \mathbf{U} \mathbf{U}) = -\nabla p + \nabla \cdot \boldsymbol{\tau} + (\rho - \rho_a) \mathbf{g}, \tag{2.2}$$

$$\frac{\partial \rho h}{\partial t} + \nabla \cdot (\rho \mathbf{U} h) = \nabla \cdot \left(\frac{\mu}{Pr_t} \nabla h \right) + Q_{FW} - S_R, \tag{2.3}$$

$$\frac{\partial \rho Y_i}{\partial t} + \nabla \cdot (\rho \mathbf{U} Y_i) = \nabla \cdot \left(\frac{\mu}{\text{Sc}_i} \nabla Y_i \right) + w_i, \quad i = 1, \dots, N-1, \quad (2.4)$$

$$\frac{\partial \rho k}{\partial t} + \nabla \cdot (\rho \mathbf{U} k) = \nabla \cdot \left(\frac{\mu}{\sigma_k} \nabla k \right) + G - \rho \varepsilon, \quad (2.5)$$

$$\frac{\nabla \rho \varepsilon}{\partial t} + \nabla \cdot (\rho \mathbf{U} \varepsilon) = \nabla \cdot \left(\frac{\mu}{\sigma_\varepsilon} \nabla \varepsilon \right) + \frac{\varepsilon}{k} (C_1 G - C_2 \rho \varepsilon), \quad (2.6)$$

$$P_a = \rho R^0 T \sum_{i=1}^N \frac{Y_i}{m_i}, \quad (2.7)$$

$$\sum_{i=1}^N Y_i = 1, \quad \sum_{i=1}^N w_i = 0, \quad (2.8)$$

where all variables are functions of cylindrical coordinates (r, z) and time t ; ρ is the density; $\mathbf{U} = (u, v)$ is the velocity vector; $\nabla \cdot \mathbf{U} = \frac{1}{r} \frac{\partial ru}{\partial r} + \frac{\partial v}{\partial z}$; P is the pressure; $p = P - P_a$ is overpressure; P_a and ρ_a are the pressure and density, respectively, of the undisturbed atmosphere; and $\mathbf{g} = (0, -g)$ is the acceleration of gravity. The gas consists of $N = 5$ components (fuel, O_2 , CO_2 , H_2O , N_2) with relative mass concentrations Y_i , thermal capacities $C_{p,i}$ and molecular weights m_i ; $h = \sum_{i=1}^N Y_i \int_{T_a}^T C_{p,i} dT$ is the enthalpy; and T is the temperature. Transport Eq. (2.4) is solved for all the components, except neutral gas (N_2), the mass fraction of which is defined from the first balance ratio (2.8). Gas law (2.7) is written in approximation of essentially subsonic flows for which $|p| \ll P_a$; the left part of (2.7) contains the pressure of the atmosphere P_a , and incomplete pressure is $P = P_a + p$. At the same time, filtered sound waves, which are insignificant for this problem, but that complicate the procedure of its numerical solution are contained in the equations.

Effective gas viscosity μ is the sum of the laminar μ_l and turbulent μ_t components. The latter is found as a function of turbulent kinetic energy k and its dissipation rate ε . The tensor of viscous pressure is expressed through the gradients of velocity and turbulent characteristics as

$$\boldsymbol{\tau} = \mu \left(\nabla \mathbf{U} + (\nabla \mathbf{U})^T - \frac{2}{3} (\nabla \cdot \mathbf{U}) \mathbf{I} \right) - \frac{2}{3} \rho k \mathbf{I}, \quad \mu = \mu_l + \mu_t, \quad \mu_t = C_\mu \rho \frac{k^2}{\varepsilon}, \quad (2.9)$$

where \mathbf{I} is a unity tensor. In the calculation of the generation rate of turbulent energy, G , the influence of the forces of buoyancy are considered:

$$G = \mu_t \left(|\nabla \mathbf{U} + (\nabla \mathbf{U})^T|^2 - \frac{2}{3} (\nabla \cdot \mathbf{U})^2 \right) - \frac{2}{3} \rho k (\nabla \cdot \mathbf{U}) + \frac{\mu_t g}{\rho} \frac{\partial \rho}{\partial z}. \quad (2.10)$$

The standard set of constants included in the composition of the turbulence model (2.5), (2.6), and (2.9) is used: $C_\mu = 0.09$, $C_1 = 1.44$, $C_2 = 1.92$, $\sigma_k = 1.0$, $\sigma_\varepsilon = 1.3$, and $\text{Pr}_t = \text{Sc}_t = 0.7$.

Fuel burning is described by the one-phasic irreversible gross reaction



where ν_i are the mass stoichiometric coefficients (here and below, as the i index, the designations of the corresponding chemical components are used; fuel is designated by the F index). The rate of turbulent burning is described by the Eddy Breakup model [12], according to which the burning rate at a high temperature does not depend on kinetic reactions and is governed exclusively by the rate of the turbulent mixing of components. The mass rate of fuel consumption per volume unit is expressed as

$$w = \rho A \frac{\varepsilon}{k} \min \left(Y_F, \frac{Y_{\text{O}_2}}{\nu_{\text{O}_2}}, \frac{B(Y_{\text{CO}_2} + Y_{\text{H}_2\text{O}})}{\nu_{\text{CO}_2} + \nu_{\text{H}_2\text{O}}} \right), \quad (2.11)$$

where $A = 4$ and $B = 0.5$. The thermal emission rate in the right part of Eq. (2.3) is equal to the product of the reaction rate (2.11) on the heating power Q_F . The rates of the formation or consumption of individual

components in Eq. (2.4) are expressed through the velocity w and mass stoichiometric coefficients such as $w_i = \pm v_i w$, where the plus sign is used for reaction products, and the minus sign for a fuel and an oxidizer; moreover, $v_F = 1$ by definition w .

Numerical solution method. Problem (2.1)–(2.11) was approximated by the method of the final volume on an orthogonal grid; at the same time, the velocity components were defined on the corresponding boundaries of the cells and other variables were defined in the centers of the cells (extended grid). The general solution procedure consists in solving the equations of movement with the pressure field computed on the previous step, with subsequent correction of the pressure and velocity for the elimination of the residual of continuity equation [13]. In contrast to the well-known SIMPLE method, at the use of the approximation of essentially subsonic flows, continuity Eq. (2.1) is not solved in an explicit form. The gas density is determined from state Eq. (2.7) by the calculated concentrations of components and temperature, whereas continuity Eq. (2.1) is used for obtaining the elliptical equation for the pressure correction. All transfer equations were approximated by the implicit scheme of the first order over time and solved by the longitudinal-transverse sweep method. The elliptical equation for the pressure correction is solved by the method of a multigrid relaxation providing uniform convergence irrespectively of the grid sizes. The calculation program is implemented in the C++ language.

Calculation of radiative heat transport and heat fluxes from a fireball. In the energy Eq. (2.3), there is a source member S_R that describes the processes of radiative heat transport. The optical properties of burning products were described by the model of the weighed sum of gray gases; the radiation transport was calculated for each gray gas either by the model of volume luminescence or on the basis of the P_1 -approximation of the spherical harmonics method (the model is described in greater detail in [11]; the solution of 2nd-order equations for radiant energy density was carried out by the multigrid method). Such an approach allows us to calculate heat transport by radiation in a fireball itself; however, both these models do not give the necessary accuracy on long distances from the fireball. Therefore, the Monte Carlo method was used for the calculation of heat fluxes and damage zones.

The Monte Carlo method is based on the modeling of processes of energy transfer by thermal radiation by tracing many representative groups of photons. The photons are distributed on the cells of a calculation grid; moreover, the number of photons in the i th cell is proportional to the energy quantity luminesced in this cell in time unit $n_i \approx k_i \sigma T_i^4 \Delta V_i$; here, k_i is the absorption factor, σ is the Stefan–Boltzmann constant, T_i is the temperature, and V_i is the volume of the i th cell. To each photon energy $Q_{ph} = k_i \sigma T_i^4 \Delta V_i / n_i$ is given, so the sum on all photons gives the total energy radiated in the calculation area in a unit of time. Then, the processes of emission, distribution, and absorption of each photon (the dispersion of radiation is not accounted for) are traced. We note that in the use of the model of the weighed sum of gray gases, the calculations are carried out for each gray gas separately, instead of for the average absorption factor for all gray gases.

The summation of the energies of all photons absorbed in a grid cell gives, after division into this cell volume, the power density of the absorbed radiation. Accordingly, the summation of all photons that crossed the cell face on the boundary of the area and division into this cell area allow us to obtain the energy flow falling on one unit of the surface in a unit of time.

Unlike the equations of hydrodynamics that are solved in a two-dimensional area for an axisymmetric problem, the calculation of radiation transfer calls for the consideration of three-dimensional geometry, and tracing the intersection points of the photon's trajectory with coordinate surfaces, which involves considerable calculations (a more detailed description of the implementation of the method can be found in [11]).

Determination of thermal radiation effects. Typically, the effect of thermal radiation from fireballs lasts for a short period of time (for typical industrial accidents, the burning time of a fireball with a fuel weight of several tons comes to about ten seconds); thus, the danger of thermal radiation depends both on the value of the thermal flow, and on the duration of the action of the thermal radiation. As investigations have shown, the effects of the impact of thermal radiation are determined by the product of heat flow raised to the power of 4/3 and the exposition time.

The influence of thermal radiation on people has not been determined, and has a stochastic nature. For example, at the set heat flow of q_s (W/m^2) and exposition time t , there is a certain probability that either a lethal outcome or merely first or second degree burns can occur. Models based on the use of probit functions are now widely applied [14, 15] for the quantitative characteristic of the probability of these or other consequences.

Probit function Pr is associated with the probability of the occurrence of the set of P_i consequences according to the following formula:

$$P_i = 50 \left[1 + \frac{Pr - 5}{|Pr - 5|} \operatorname{erf} \left(\frac{|Pr - 5|}{\sqrt{2}} \right) \right], \quad (2.12)$$

where probability P_i is expressed in percentage terms. The relation between characteristics of influence and probit functions is set separately for different consequences. For the nonstationary influence of thermal emission, the following ratios are cited in the literature: the probability of receiving first degree burns corresponds to the probit function $Pr_I = -39.83 + 3.0186 \ln(q_s^{4/3} t)$; the probability of receiving second degree burns corresponds to the probit function $Pr_{II} = -43.14 + 3.0188 \ln(q_s^{4/3} t)$; the probability of a lethal outcome for people unprotected with special suits corresponds to the probit function $Pr_L = -36.38 + 2.56 \ln(q_s^{4/3} t)$ (in these formulas the heat flow q_s is measured in W/m^2 , and exposition time t is measured in seconds).

The application of the specified formulas for probit functions to the numerical calculations becomes complicated by the fact that the flows found in the calculations are not constant in time. Actually, according to the calculations, the thermal dose $I_s = \int_0^t q_s(\tau) d\tau$, expressed in J/m^2 is formed. Therefore, for the calculation of probit functions, the following approximation is accepted: $q_s^{4/3} t \approx I_s^{4/3} t_{FB}^{-1/3}$, where t_{FB} is the burning time of a fireball, defined on the dependence of the aggregate rate of thermal emission on time.

RESULTS OF THE NUMERICAL MODELING OF THE BURNING OF AIR-GAS FUEL CLOUDS

Numerical Modeling of a Fireball During the Burning of 2 Tons of Butane

This scenario corresponds to the parameters of natural field test [16] in which a fireball was formed at the destruction of a tank with liquefied butane with a fuel weight M_0 of 2000 kg. The tank's content was preliminarily heated up to 100°C ($T_0 = 373 \text{ K}$, which corresponds to a pressure of saturated steam of $P_0 = 15 \text{ bar}$). The calculations were carried out on complex grids containing 100×200 cells in the radial and vertical directions.

After depressurization on a Boiling Liquid Expanding Vapor Explosion (BLEVE) mechanism, the fuel scatters after mixing with the surrounding air. The arising fuel-air cloud is lit up near a fuel source; as a result, there is a fireball in the atmosphere. In the numerical calculations, the initial conditions were set by the results of modeling the cloud formation process at the instant of the destruction of the tank. Then, during a short time ($\Delta t_i = 0.5 \text{ s}$), the calculation was carried out without ignition; for this time, there was a coordination of fields of variables and additional mixing of fuel with the air due to turbulent diffusion. On the termination of this stage, fuel located in the center located at the beginning of the coordinates was ignited.

In Fig. 3, the structure of the burning cloud during time $t = 1\text{--}8 \text{ s}$ after ignition is shown.

The field of temperatures is shown for each instant by isolines, and the velocity field is shown by vectors. The ignition of the fuel-air mixture formed in the cloud center leads at the initial stage to a radial distribution of the burning wave on the mixed gas mixture ($t = 1 \text{ s}$). The velocity field also has a radial character at this stage, corresponding to simple gas expansion. Since the cloud is excessively rich in fuel, in the burning wave that is spreading into the cloud, the oxygen burns out, and the remainder of the fuel burns down in diffusive mode, after mixing with oxygen on the external cover of the fireball. Under the influence of buoyancy forces, hot products start to flow upwards, the velocity field gets a vortex character, and the hemispherical cloud comes off the earth and is transformed into a mushroom-shaped fireball ($t = 4 \text{ s}$). As the fuel burns the gas temperature falls, and the products rise into the atmosphere as thermal ones ($t = 8 \text{ s}$).

The integral characteristics of the fireball obtained in the calculations are highly coordinated with the experimental data of work [16]. Thus, the maximal diameter of the fireball defined by the isotherm $T = 500 \text{ K}$ came to 80 m in the calculations, and in the experiments it came to 85 m. The time of the takeoff of the fireball came to 3 s, and in the experiments it came to 3.6 s; the total time of burning was 7 s, while in the experiments it was 6.5 s.

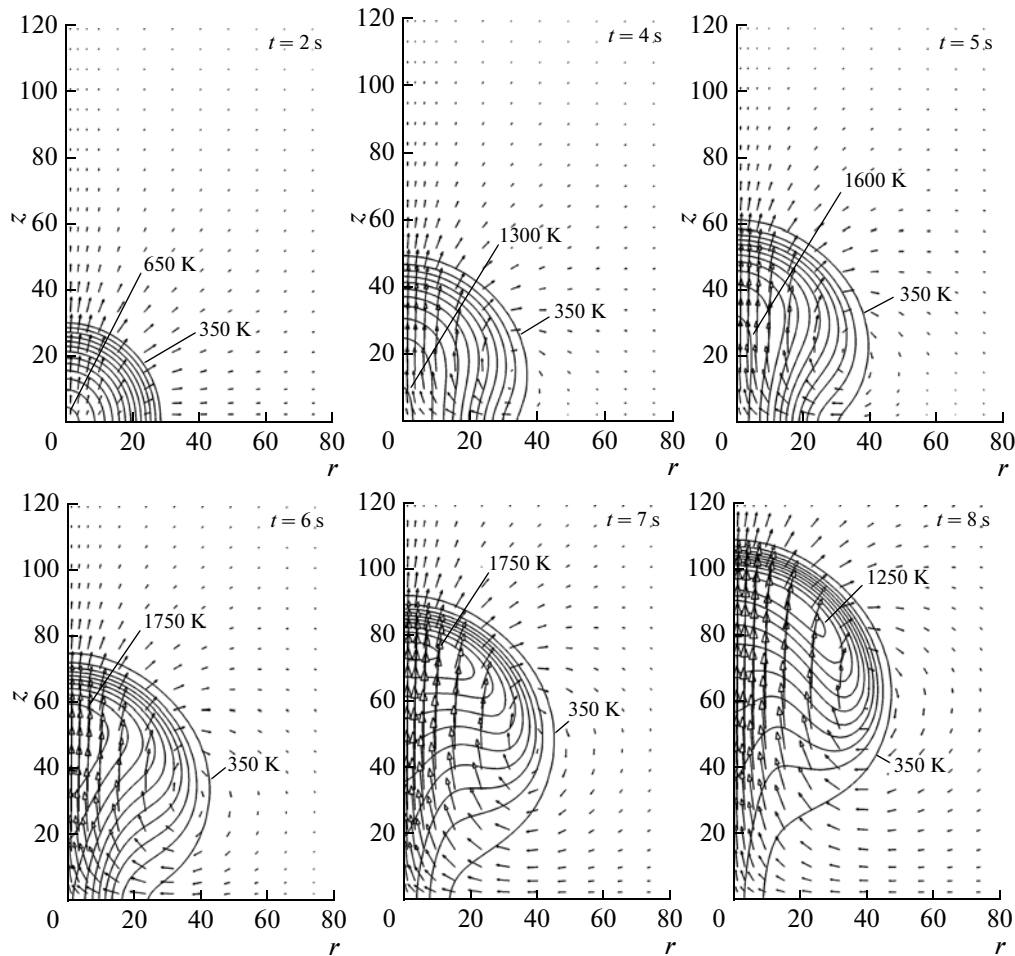


Fig. 3. Structure of the burning cloud at the complete destruction of a tank containing liquefied butane with a fuel weight equal to $M_0 = 2 \times 10^3$ kg at different times.

For this experiment, the total energy of fuel combustion comes to $Q_{\text{tot}} = 9.15 \times 10^{10}$ J. The calculated dependences of thermal emission rates dQ/dt (where Q is the energy of the fuel combustion, isolated at time t), and the share of the total released energy Q/Q_{tot} (the latter magnitude also characterizes the share mass of the fuel that burned in the fireball up to time t) in time are presented in Fig. 4. The total duration of the fireball burning for these parameters of the problem comes to $t_{FB} = 7.5$ s (taking into account the ignition delay Δt_i ; in time t_{FB} , 95% of the fuel weight burns off).

In Fig. 5, the radial distributions of the heat fluxes from the fireball in different times $q_s(r, t)$, and also the radial distribution of the thermal dose $I_s(r)$ obtained by the integration of the heat fluxes in time are presented. For both graphs, the logarithmic scale on the Y axis is used. It is clear that at the initial stage of burning when the fireball touches the ground, the most intensive heat fluxes are reached directly under the fireball itself. As the burning cloud increases in size and rises from the ground, the heat flow appears to be distributed along the radius more evenly. After the burning off of most of the fuel, the heat fluxes are sharply weakened.

The probabilities of damages of varying degrees can be obtained according to the calculated thermal dose and time of existence of the fireball by means of the probit function (2.12). In Fig. 6, the radial distributions are constructed of the probability of first and second degree burns, as well as the probability of a lethal outcome, from the influence of the thermal radiation of a fireball (the probabilities of a damage are expressed in percentage terms), and the corresponding zones of damage are presented in Fig. 7. We note that in this work the heat fluxes on a horizontal surface are calculated. The probability of a damage for standing person can be found similarly, but it requires special calculations.

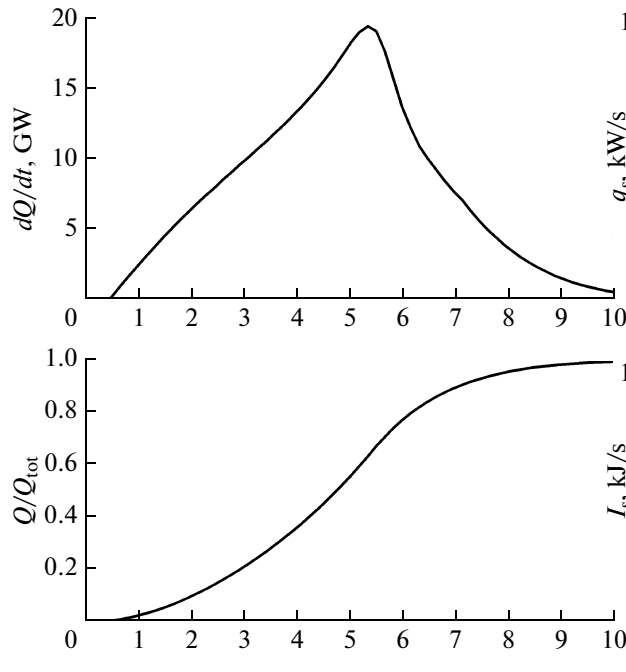


Fig. 4. Dependences of the thermal emission rate dQ/dt (upper figure) and the share of the released heat Q/Q_{tot} (lower figure) on time at the burning of a butane fireball with fuel weight $M_0 = 2 \times 10^3$ kg.

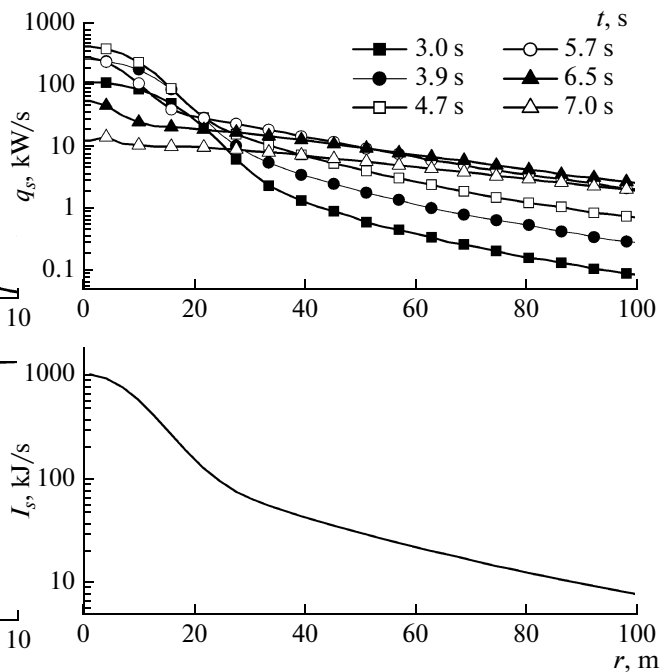


Fig. 5. Radial distributions of heat fluxes q_s from a fireball at the burning of 2×10^3 kg of butane at different times (upper figure) and the distribution of a thermal dose on the surface I_s (lower figure).

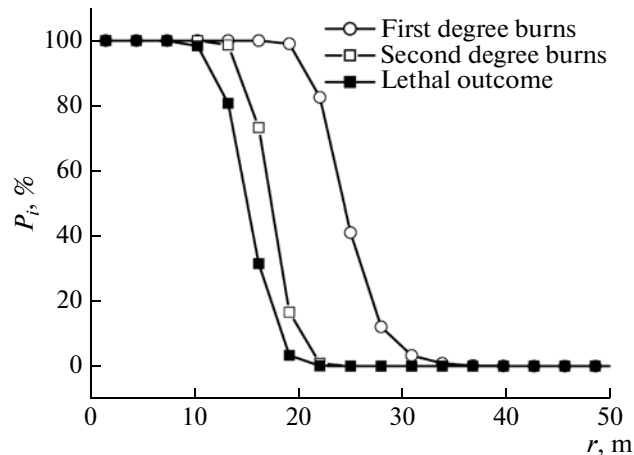


Fig. 6. Probability of damages of different degrees from the thermal radiation of a fireball with a butane weight of $M_0 = 2 \times 10^3$ kg.

Numerical Modeling of a Fireball at the Burning of 50 Tons of Butane

For this scenario, the total energy of fuel combustion in a fireball ($M_0 = 5 \times 10^4$ kg) comes to $Q_{tot} = 2.29 \times 10^{12}$ J. Qualitatively, the evolution of the fireball is similar to the one presented in Fig. 3 for a smaller fuel weight—in the burning process, the initial hemispherical cloud transforms into a mushroom-shaped fireball.

The calculated dependences of thermal emission rates dQ/dt and the share of total released energy Q/Q_{tot} over time t are presented in Fig. 8. The total duration of the fireball's burning for these parameters comes to $t_{FB} = 15$ s (taking into account the ignition delay Δt_i ; in time t_{FB} , 95% of the fuel mass burns off). The radial distributions of heat fluxes from the fireball in different times $q_s(r, t)$ and also the radial distribution of a thermal dose $I_s(r)$ obtained by the integration of heat fluxes in time are presented in Fig. 9. For

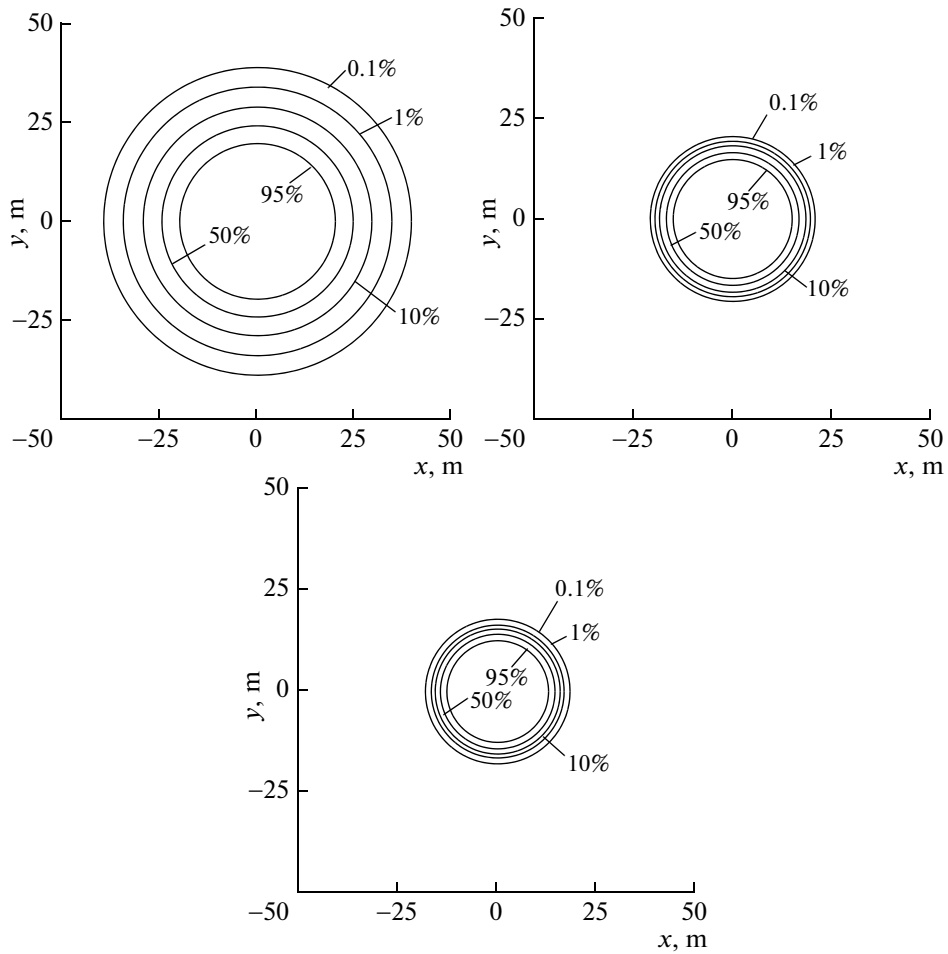


Fig. 7. Damage zones of different degrees at the burning of 2×10^3 kg of butane (from left to right): first degree burns, second degree burns, and lethal outcome. In every figure, five concentric circles corresponding to the damage probabilities 0.1, 1, 10, 50 and 95%.

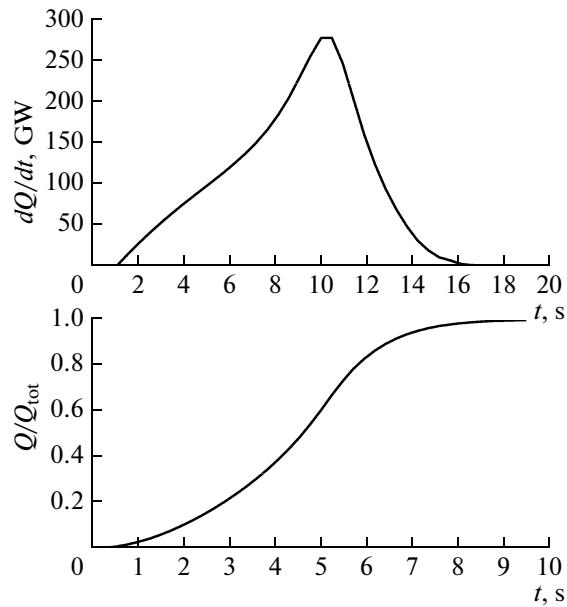


Fig. 8. Dependences of the thermal emission rate dQ/dt (upper figure) and share of released heat Q/Q_{tot} (lower figure) on time at the burning of a butane fireball with a fuel weight $M_0 = 5 \times 10^4$ kg.

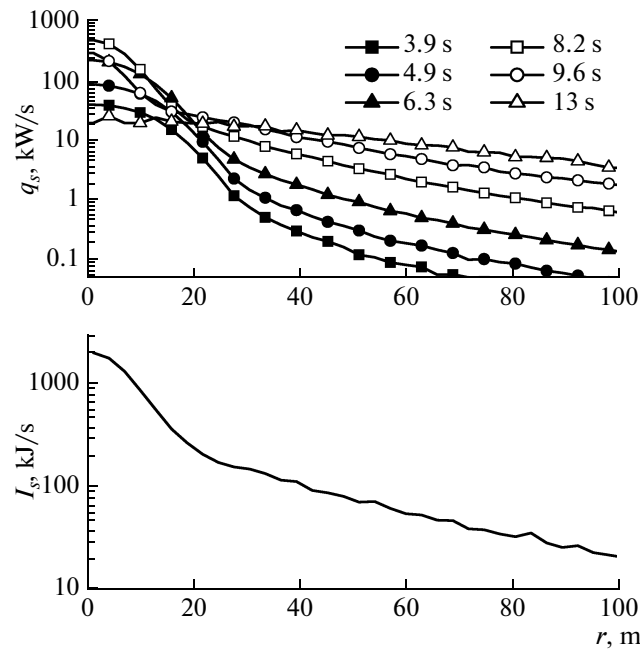


Fig. 9. Radial distributions of heat fluxes q_s from a fireball at the burning of 5×10^4 kg of butane at different times (upper figure) and the distribution of a thermal dose on the surface I_s (lower figure).

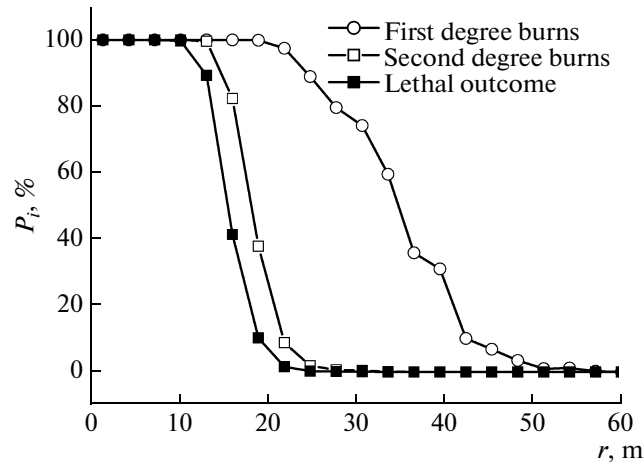


Fig. 10. Probability of damages to different degrees from the thermal radiation of a fireball of mass $M_0 = 5 \times 10^4$ kg.

both graphs the logarithmic scale on the Y axis is used. It is clear that at the initial stage of burning when the fireball touches the ground, the most intensive heat fluxes rise directly under the fireball itself. As the burning cloud increases in size and leaves the ground, the heat flow appears to be distributed along the radius more evenly. After most of the fuel is burned off, the heat fluxes are sharply weakened.

The radial distributions of the probability of first and second degree burns, and also a lethal outcome from the influence of the thermal radiation of the fireball (the probabilities of damage are expressed in percentage terms) are constructed in Fig. 2.8. As well as the previous calculation, due to the short duration of the heat impulse, the probable zone of receiving second degree and deadly burns is located in the immediate proximity of an accident, whereas the probable zone of receiving first degree burns for a fuel weight of 50 t is much more extensive (for example, a zone radius corresponding to a 10% probability comes to 43 m, whereas for a fuel weight of 2 t, it came to 28 m).

CONCLUSIONS

The mathematical models presented in the present work and the software created on their basis allow us to model accidents with the distribution of toxic gas clouds over an area with a complex relief, and also accidents with the burning of fuel-air clouds in the mode of a fireball. The given examples of calculations of the development of an accident with chlorine emission in the conditions of a city building construction and butane fireball show that on the basis of these models and software tools, it is possible to estimate the areas of toxic and thermal damage. The used two-dimensional approximation considerably reduces computing expenses, which has resulted in these models becoming suitable for use both in scientific research and engineering practice in the estimation of the dangers and risks of technogenic accidents.

REFERENCES

1. V. C. Marshall, *Major Chemical Hazards* (Ellis Horwood, Chichester; 1987; Mir, Moscow, 1989).
2. O. V. Dobrocheev, A. A. Kuleshov, N. P. Savenkova, and S. V. Filippova, "2D Model of Heavy Gases Dispersion on Orographically Inhomogeneous Earth Surface," *Mat. Model.* **8**, No. 5, 91–105 (1996).
3. A. A. Kuleshov, "Mathematical Simulation in the Problems of Industrial Security and Ecology," *Inf. Tekhnol. Vychislit. Sist.*, No. 4, 56–70 (2003).
4. J. J. Stoker, *Water Waves, The Mathematical Theory with Applications* (Interscience, New York, 1957; Inostr. lit, Moscow, 1959).
5. I. E. Penner, L. C. Haselman, and L. L. Edwards, "Buoyancy Plume Calculation," *AIAA Pap.*, No. 459, 1–9 (1985).
6. I. V. Vorontsov and A. K. Yanushevskii, et al., *Guidance Documents on Elimination of Medical and Health Consequences of the Chemical Accidents* (Vserossiiskii Tsentri Meditsiny Katastrof "Zashchita", 2001) [in Russian].
7. *Chemical Weapons of Potential Adversary*, Ed. by A. N. Kalitaev (Izd-vo Voennoi akad. khim. zashchity, Moscow, 1977) [in Russian].
8. G. M. Makhviladze, J. P. Roberts, and S. E. Yakush, "Combustion of Two-Phase Hydrocarbon Fuel Clouds Released Into the Atmosphere," *Combust. Flame* **118**, 583–605 (1999).
9. G. M. Makhviladze and S. E. Yakush, "Modeling of Formation and Combustion of Accidentally Released Fuel Clouds. Hazards XVIII: Process Safety—Sharing Best Practice," *ICHEME Symp. Ser.* **150** 106 (2004).
10. G. M. Makhviladze, J. P. Roberts, and S. E. Yakush, "Fire Ball during Burning of Hydrocarbon Fuel Blowouts. I: Rise Structure and Dynamics," *Fiz. Goreniya Vzryva* **35**, No. 3, 7–19 (1999).
11. G. M. Makhviladze, J. P. Roberts, and S. E. Yakush, "Fire Ball during Burning of Hydrocarbon Fuel Blowouts. II: Heat Radiation," *Fiz. Goreniya Vzryva* **35**, No. 4, 12–23 (1999).
12. B. F. Magnussen and B. H. Hjertager, "On the Mathematical Modeling of Turbulent Combustion with Special Emphasis on Soot Formation and Combustion," in *Proc. 16th Int. Symp. on Combustion* (The Combustion Inst., Pittsburgh, PA, 1976), pp. 711–729.
13. G. M. Makhviladze and V. I. Melikhov, "Method for Numerical Researching of Gases Slow Combustion," *Mat. Model.* **1**, No. 6, 146–157 (1989).
14. *Russian National Security. Law, Socio-Economic and Scientific-Technical Aspects* (MGF "Znanie", Moscow, 1998), Part 1, pp. 192–195 [in Russian].
15. *CCPS Guidelines for Chemical Process Quantitative Risk Analysis* (American Institute of Chemical Engineers, New York, 2000).
16. D. M. Johnson and M. J. Pritchard, "Large-Scale Experimental Study of Boiling Liquid Expanding Gas Explosions (BLEVEs)," in *14th Int. LNG/LPG Conf. & Exhibition Gastech'90* (Amsterdam, 1990), pp. 1–30.